

SUPPLEMENTARY INFORMATION

For

**Ni-substituted LaMnO<sub>3</sub> Perovskites for Ethanol Oxidation**

Yi-Chen Hou, Ming-Wei Ding, Shih-Kang Liu, Shin-Kuan Wu, and Yu-Chuan Lin\*

Department of Chemical Engineering and Materials Science  
Yuan Ze University, Chungli, Taoyuan 32003, Taiwan

---

\* Corresponding author's Tel.: (886) 3 463 8800 ext. 3554; Fax: (886) 3 455 9373; email:  
[yclin@saturn.yzu.edu.tw](mailto:yclin@saturn.yzu.edu.tw)

## Content

### Table

Table S1. Reduction properties of  $\text{LaMn}_{1-y}\text{Ni}_y\text{O}_3$  catalysts.

### Figures

Fig. S1. C 1s core level spectra of  $\text{LaMn}_{1-y}\text{Ni}_y\text{O}_3$  perovskites.

Fig. S2. XRD patterns of post-TPR samples.

Fig. S3. TPR profiles of physically mixed  $\text{LaMnO}_3$  and  $\text{LaNiO}_3$  particles.

Fig. S4. The variations of XPS-derived Ni loading (%), amounts of  $\alpha$ - and  $\beta$ -oxygen ( $\mu\text{mol/g cat.}$ ), and  $T_{50}$  and  $T_{95}$  ( $^\circ\text{C}$ ) of testes  $\text{LaMn}_{1-y}\text{Ni}_y\text{O}_3$  as functions of  $y$  values.

Fig. S5. Conversion of ethanol as a function of temperature over physically mixed  $\text{LaMnO}_3$  and  $\text{LaNiO}_3$  particles.

Fig. S6. Acetaldehyde and carbon dioxide selectivities as functions of temperature over physically mixed  $\text{LaMnO}_3$  and  $\text{LaNiO}_3$  particles.

Fig. S7. SEM images of as-synthesized and used  $\text{LaMn}_{1-y}\text{Ni}_y\text{O}_3$ .

Table S1. Reduction properties of  $\text{LaMn}_{1-y}\text{Ni}_y\text{O}_3$  catalysts.

catalyst		TPR test		
		$T_{\text{low peak}}^{\text{a}}$	$T_{\text{high peak}}^{\text{b}}$	$T_{\text{high}}/T_{\text{low}}$
y = 0	T (°C)	337	747	
	mmol/g cat.	1.23 (40%)	1.83 (60%)	1.5
y = 0.1	T (°C)	335	783	
	mmol/g cat.	0.92 (31%)	2.05 (69%)	2.2
y = 0.25	T (°C)	397	738	
	mmol/g cat.	1.35 (37%)	2.33 (63%)	1.7
y = 0.4	T (°C)	359	736	
	mmol/g cat.	1.29 (33%)	2.63 (67%)	2.0
y = 1	T (°C)	347	469	
	mmol/g cat.	3.08 (51%)	3.01 (49%)	1.0

<sup>a</sup> Maximum temperature of reduction peak below 500 °C except  $\text{LaNiO}_3$  (y = 1), which used 400 °C as the demarcation.

<sup>b</sup> Maximum temperature of reduction peak above 500 °C except  $\text{LaNiO}_3$  (y = 1), which used 400 °C as the demarcation.

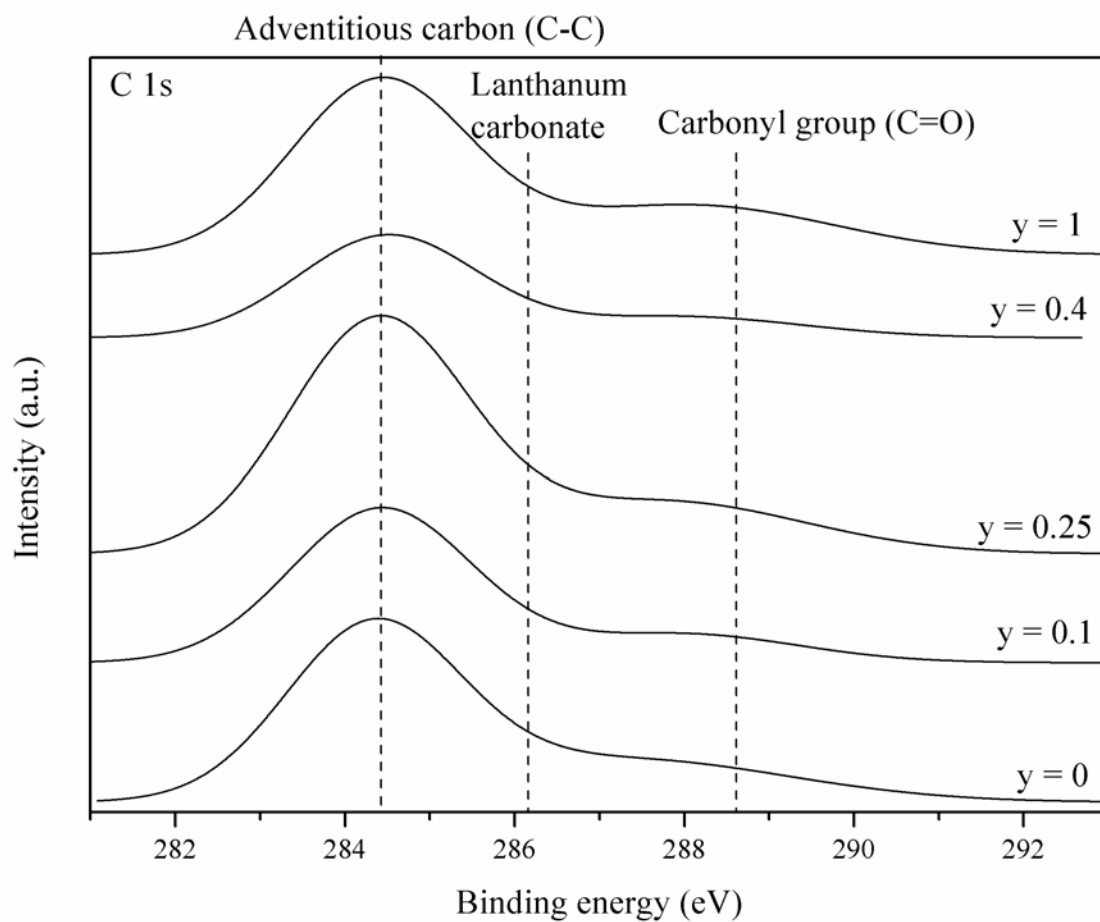


Fig. S1. C 1s core level spectra of LaMn<sub>1-y</sub>Ni<sub>y</sub>O<sub>3</sub> perovskites.

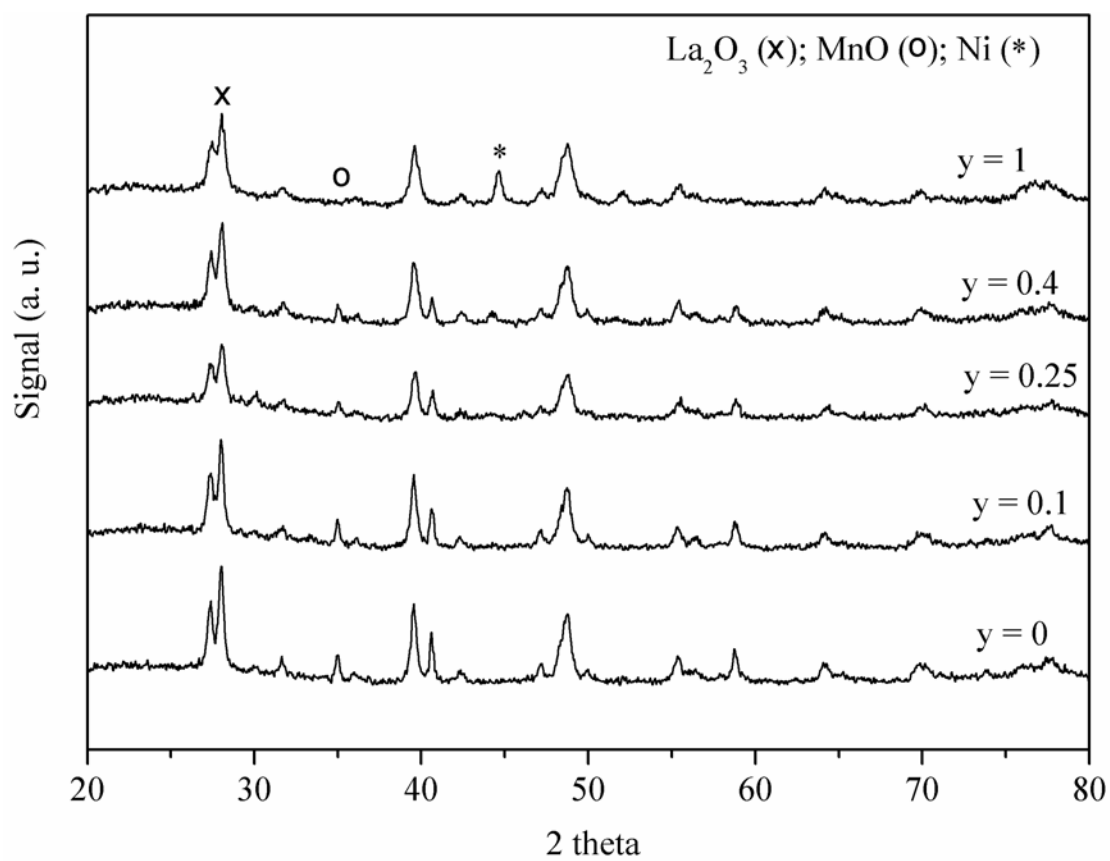


Fig. S2. XRD patterns of post-TPR samples.

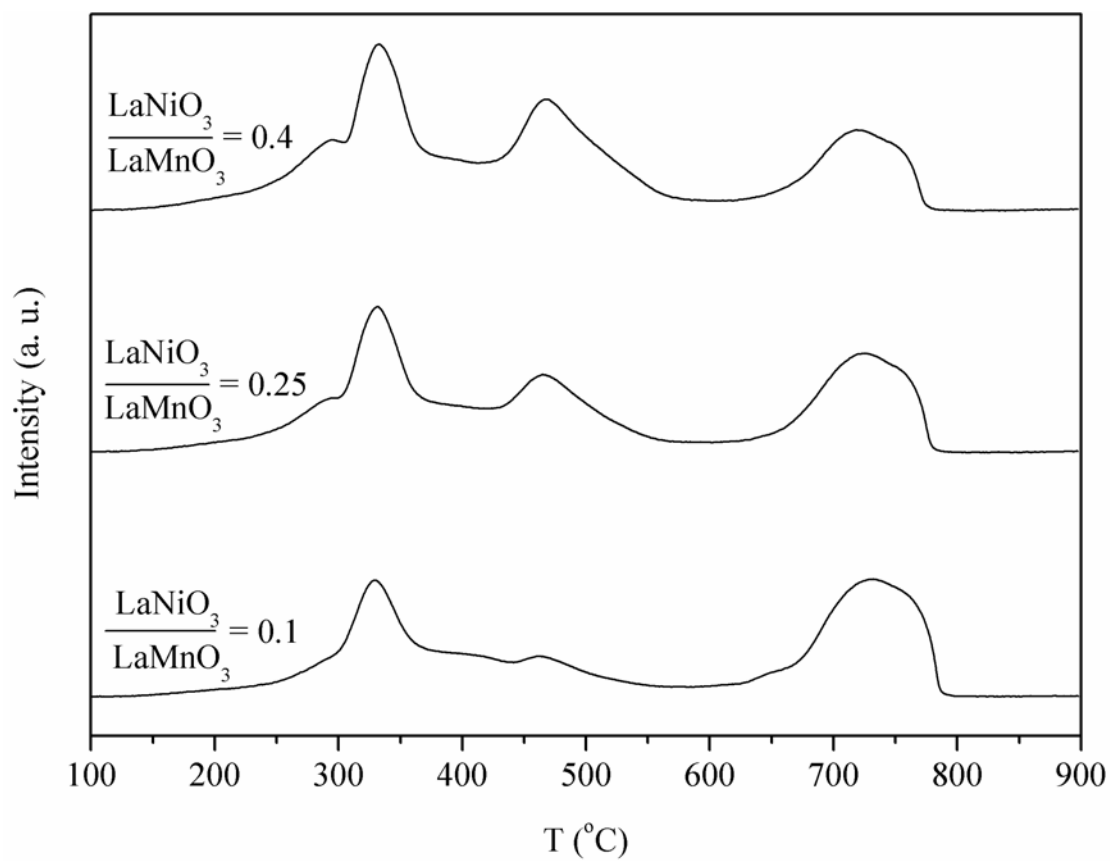


Fig. S3. TPR profiles of physically mixed  $\text{LaMnO}_3$  and  $\text{LaNiO}_3$  particles.

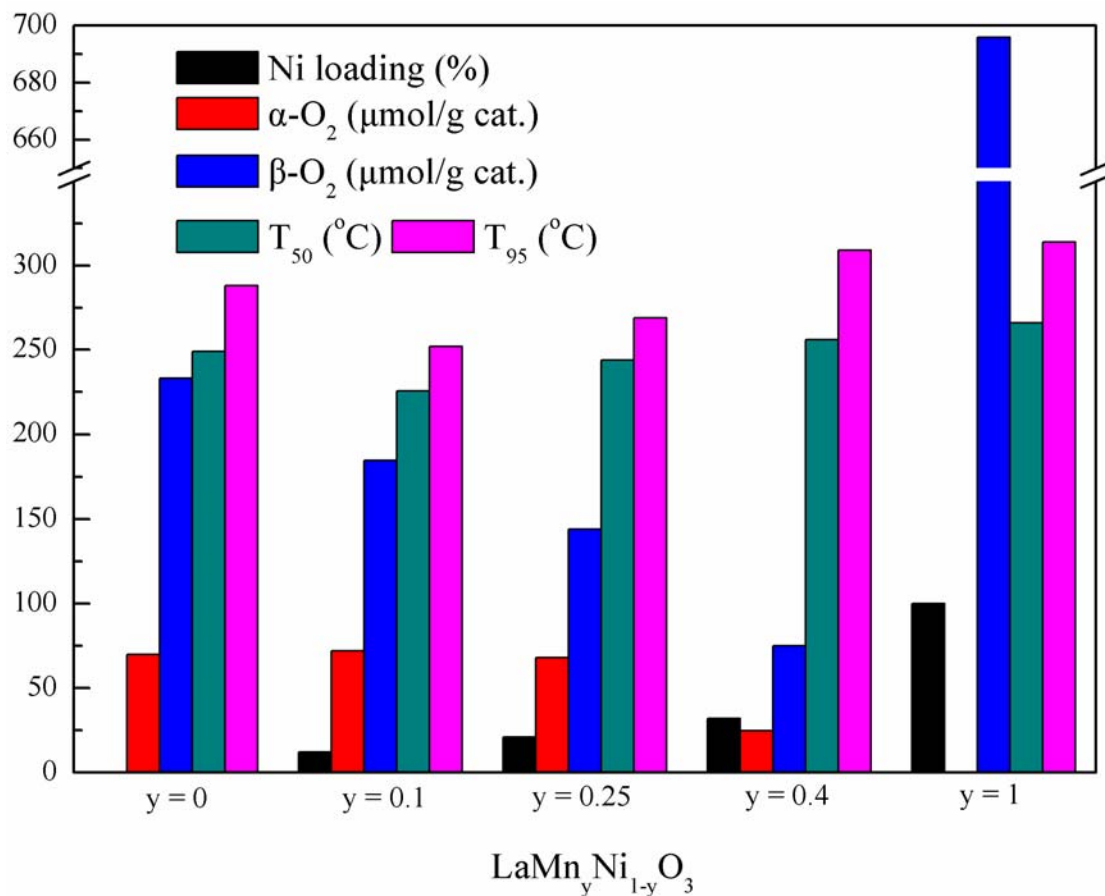


Fig. S4. The variations of XPS-derived Ni loading (%), amounts of α- and β-oxygen (μmol/g cat.), and T<sub>50</sub> and T<sub>95</sub> (°C) of testes LaMn<sub>1-y</sub>Ni<sub>y</sub>O<sub>3</sub> as functions of y values.

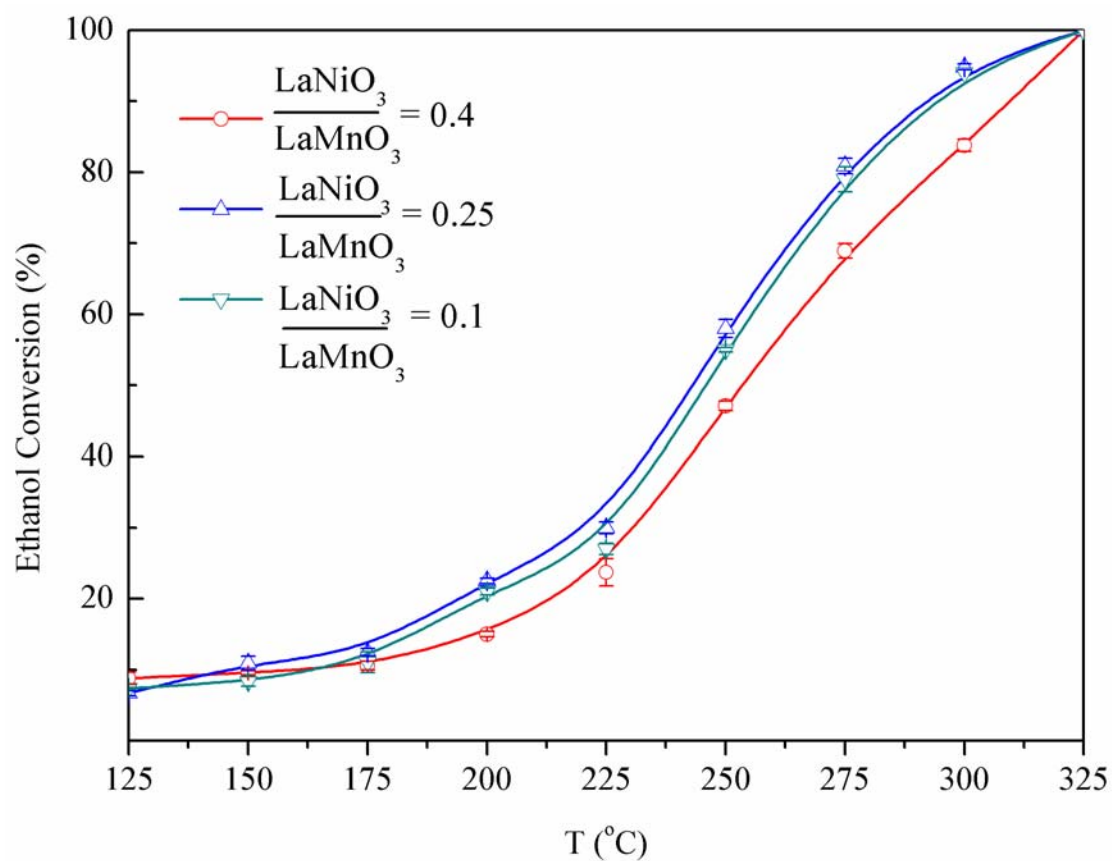


Fig. S5. Conversion of ethanol as a function of temperature over physically mixed LaMnO<sub>3</sub> and LaNiO<sub>3</sub> particles.

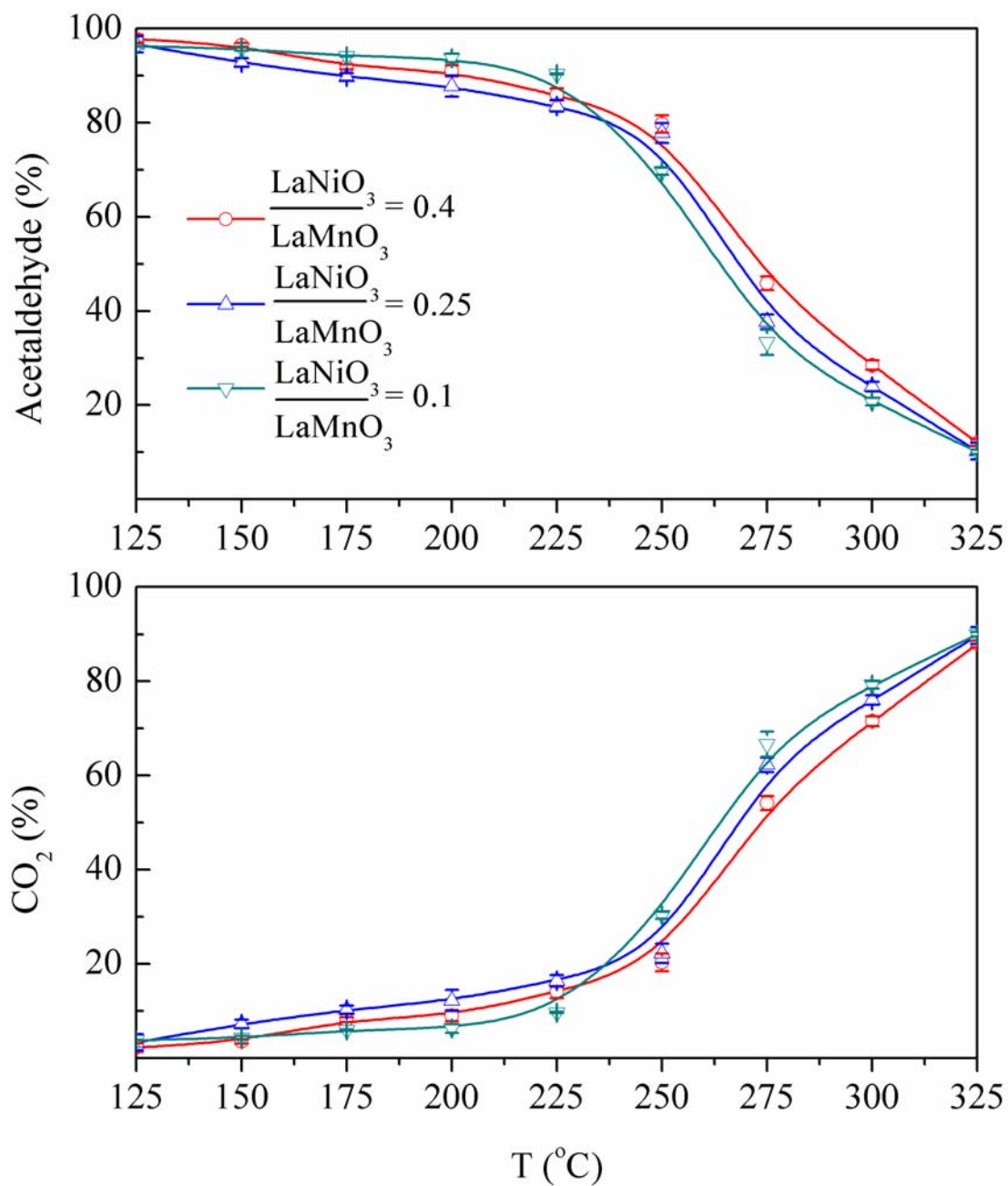


Fig. S6. Acetaldehyde and carbon dioxide selectivities as functions of temperature over physically mixed  $\text{LaMnO}_3$  and  $\text{LaNiO}_3$  particles.

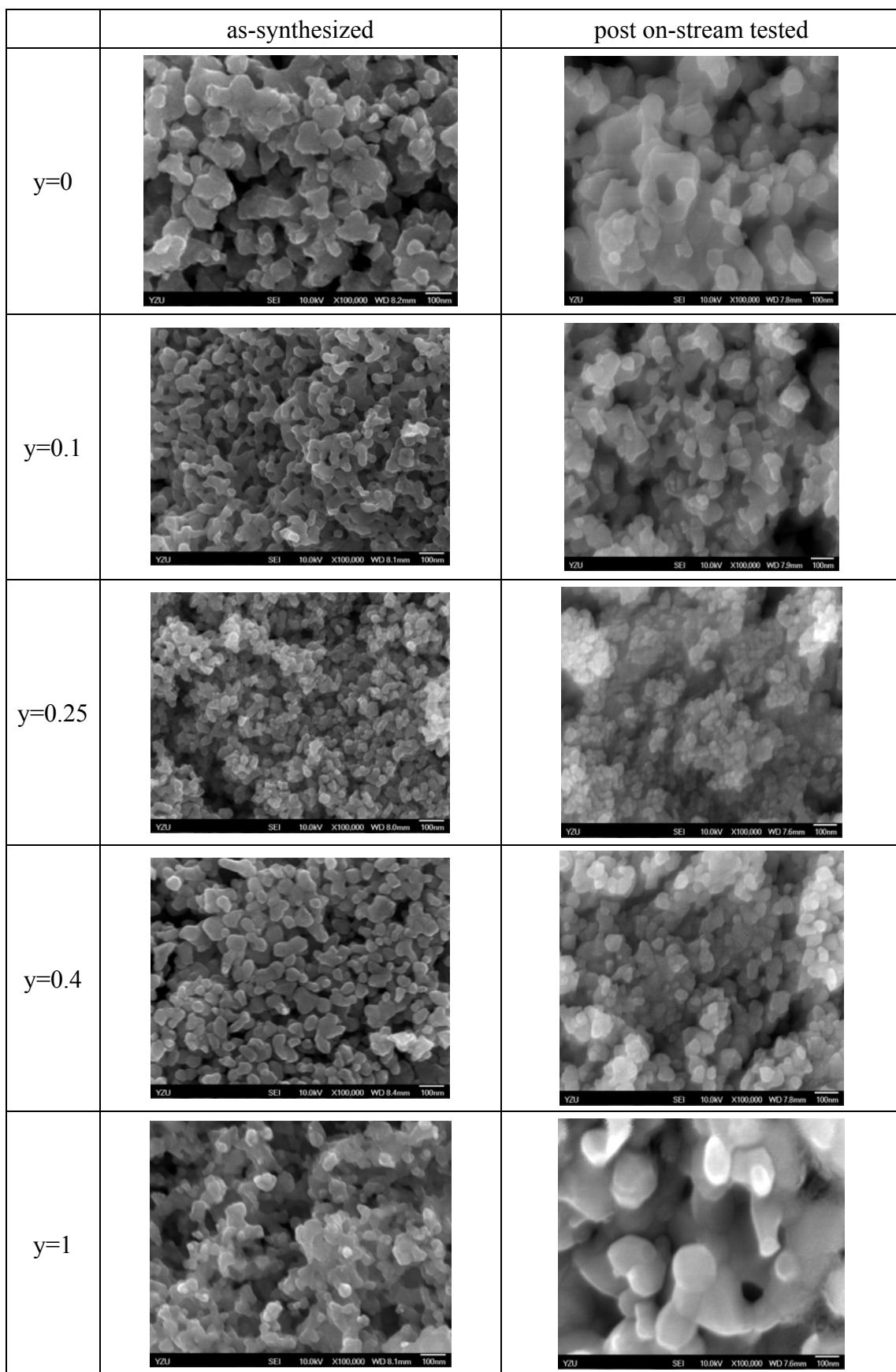


Fig. S7. SEM images of as-synthesized and used  $\text{LaMn}_{1-y}\text{Ni}_y\text{O}_3$ .